Chemical Papers (2025) 79:5733–5746
https://doi.org/10.1007/s11696-025-04149-7

ORIGINAL PAPER

Bio-activity guided isolation of 1,5-dicaffeoyl quinic acid from *Cirsium* species and investigation of their therapeutic potency on melanoma through in vitro and in silico approaches

Sila Ozlem Sener[1] · Seyda Kanbolat[2] · Merve Badem[2] · Ufuk Ozgen[3] · Rezzan Aliyazicioglu[2] · Esma Ceylan[4] · Ahmet Ceyhan Goren[5,6] · Tuncay Dirmenci[7] · Turan Arabaci[8] · Sermet Yildirmis[2] · Seyma Emiroglu[3] · Gulcin Saltan İscan[9]

Received: 12 September 2024 / Accepted: 6 May 2025 / Published online: 24 June 2025

Abstract

Melanoma exhibits a high fatality rate, and its characteristic of rapid proliferation is progressively increasing. Collagenase inhibitors are pivotal in influencing the invasion of cancer cells in melanoma. The objective of this research is to explore the therapeutic impact of specific *Cirsium* species on melanoma. A bioactivity-guided fractionation was carried out to identify the effective compound using collagenase inhibitory efficacy. The most potent compound underwent additional examination through in silico methods, and the presence of this compound, along with several phenolic compounds, in the most effective *Cirsium* species was identified using LC–MS/MS analysis. The cytotoxic effect on SK-Mel cells was assessed using the in vitro MTT technique. The bioactivity-guided fractionation study led to the identification of CTR-E1 from *Cirsium trachylepis*'s root (CTR), and its structure was determined as 1,5-dicaffeoylquinic acid. In silico analysis revealed that 1,5-dicaffeoylquinic acid exhibited significant potency with a maximum binding affinity of − 8.19 kcal/mol, as well as hydrogen bonds and hydrophobic interactions. 1,5-dicaffeoylquinic acid, fumaric acid, pyrogallol, and epicatechin were detected and quantified in CTR by LC–MS/MS analysis. CTR was found to be effective on SK-Mel cells. Further clinical and toxicological studies, as well as additional in vitro and in vivo studies, are necessary to support the therapeutic efficacy of CTR and 1,5-dicaffeoylquinic acid.

Keywords 1,5-dicaffeoylquinic acid · Bio-activity-guided fractionation · *Cirsium* · Collagenase · In silico · LC–MS/MS · Melanoma

✉ Sila Ozlem Sener
silaozlem.sener@sbu.edu.tr

[1] Department of Pharmacognosy, Gulhane Faculty of Pharmacy, University of Health Sciences Turkey, Ankara, Turkey

[2] Department of Biochemistry, Faculty of Pharmacy, Karadeniz Technical University, Trabzon, Turkey

[3] Department of Pharmacognosy, Faculty of Pharmacy, Karadeniz Technical University, Trabzon, Turkey

[4] Department of Biology, Faculty of Sciences, Karadeniz Technical University, Trabzon, Turkey

[5] Department of Chemistry, Faculty of Sciences, Gebze Technical University, Gebze, Kocaeli, Turkey

[6] Troyasil HPLC Column Technologies, Umraniye, Istanbul, Turkey

[7] Department of Biology Education, Necatibey Education Faculty, Balıkesir University, Balıkesir, Turkey

[8] Department of Pharmaceutical Botany, Faculty of Pharmacy, Inonu University, Malatya, Turkey

[9] Department of Pharmacognosy, Faculty of Pharmacy, Ankara University, Ankara, Turkey

Introduction

Melanoma, a malignancy of melanocytes, has been known for its deadly effect and rapidly rising expansion compared with other cancer types (Popescu et al. 2022; AlQathama et al. 2015). It was estimated that melanoma accounts for 1.7% of all cancer types, with 325,000 new cases in 2020. According to the scientists' estimates, by 2040, there will be more than 500,000 new instances of melanoma each year and about 100,000 fatalities from the disease globally (Arnold et al. 2022; Saginala et al. 2021).

Nowadays, natural sources have become popular because of their therapeutic potential for melanoma through supporting caspase activity, reducing angiogenesis, and inhibiting tumor-promoting proteins like matrix metalloproteinases (MMPs) (Chinembiri et al. 2014). Collagenases belonging to the MMP family can degrade the collagenous extracellular matrix. The growth and metastasis of cancer cells have been proven to be significantly influenced by collagenases (Ala-aho and Kähäri 2005; Brown 1997; Zhang et al. 2004). Collagenase inhibitors have a crucial role in the treatment of melanoma since the invasion and metastasis of melanoma require the proteolytic activity of collagenase (Lida and McCarthy 2007; Napoli et al. 2020; Hofmann et al. 2005). Interstitial collagenase, MMP-1, is one of the MMPs that assists melanoma invasion through the disintegration of dermal collagen type 1. Besides, MMP-1 promotes activation of the G-protein coupled receptor Protease Activated Receptor-1 (PAR-1), thus leading to melanoma progression via activation of signal transduction pathways (Blackburn et al. 2009).

Cirsium genus is represented by 69 species (81 taxa) in Turkey (Duman et al. 2017; Dirmenci et al. 2020). *Cirsium* genus has been used as an anticancer, anxiolytic, anti-inflammatory, antihypertensive, hemostatic, and diuretic agent traditionally (Llorent-Martínez et al. 2020; Yeşilada et al. 1995). *Cirsium* genus includes phenylpropanoid glycosides, flavonoids, triterpenes, phenolic acids, and healthy fatty acids (Inafuku et al. 2013; Kozyra et al. 2013).

The present study aims to perform bio-activity-guided fractionation studies on six endemic *Cirsium* species for Turkey guidance with in vitro collagenase inhibition, to uncover the most effective compound, and then to investigate the therapeutic potential of the most effective species for skin cancer by in vitro cell line and in silico techniques.

Experimental

Materials

Chemicals and reagents

Normal phase (Silica gel 60, Cas No: 7631-86-9, Merck), octadecyl phase (C18) (LiChroprep® RP-18, Cas No: 108688-10-4, Merck), thin layer chromatography plate (TLC Silica gel 60 F254, Merck), Sephadex (Sephadex® LH-20, Cas no: 17-0090-01, Sigma-Aldrich); CH_3OH, EtOAc, and $CHCl_3$ purchased from Sigma-Aldrich (St. Louis, USA) were used for bio-activity guided fractionation studies. For in vitro cell line studies, human melanoma (SK-Mel) cell line and human fibroblast (NHDF) cells were purchased from ATCC and Sigma-Aldrich respectively, Gentamicin (Cas No: 1405-41-0, Sigma-Aldrich), fungizone (Cas No: 1397-89-3, Sigma-Aldrich), L-glutamine (Cas No: 56-85-9, Sigma-Aldrich), trypsin/EDTA (Cas No: 9002-07-7, Sigma-Aldrich); fetal bovine serum (FBS, SKU: F2442, Sigma-Aldrich), Eagle's minimum essential medium (alfa-MEM, SKU: M4655, Sigma-Aldrich), RPMI 1640 medium (Cat No: 21875-034, Thermo Fisher), 3-(4,5-dimethyl-2-thiazolyl)-2,5-diphenyl-2H-tetrazolium bromide (MTT, Cas No: 298-93-1, Sigma-Aldrich), dimethyl sulfoxide (DMSO, Cat No: 67-68-5, Sigma-Aldrich) were used for in vitro cytotoxic activity studies.

For collagenase inhibition studies, collagenase (Type I, EC232-582-9), N-[3-(2-Furyl)acryloyl]-Leu-Gly-Pro-Ala (FALGPA) (Cas No: 78832-65-2), Tris-HCl (Cas No: 1185-53-1) and epigallocatechin gallate (EGCG) (Cas No:989-51-5) were purchased from Sigma-Aldrich (St. Louis, USA).

The compounds listed below were utilized as standards in the LC–MS/MS analysis: 1,5-Dicaffeoylquinic acid (%95, Chengdu Biopurify Phytochemicals), Chlorogenic acid (90%, Sigma-Aldrich), (-)-Epicatechin (98%, Sigma-Aldrich), Epigallocatechin gallate (95%, Sigma-Aldrich), Fumaric acid (99%, Sigma-Aldrich), Gallic acid (97%, Sigma-Aldrich), Kaempferol (96%, Sigma-Aldrich), Luteolin (%98, Sigma-Aldrich), Luteolin-5-O-glu (95%, AppliChem), Luteolin-7-O-glu (95%, AppliChem), Pelargonin chloride (90%, Sigma-Aldrich), Pyrogallol (%90, Sigma-Aldrich), Quercetin (95%, Sigma-Aldrich). HPLC-grade methanol was purchased from Merck (Darmstadt, Germany).

Plant material

The aerial parts and roots of *Cirsium aristatum* DC. (CA), *Cirsium dirmilense* R.M. Burton (CD), *Cirsium elodes* M. Bieb. (CE), *Cirsium pseudocreticum* (P.H. Davis & Parris) Yıldız, Dirmenci & Arabacı (CP), *Cirsium sivasicum* Yıldız, Arabacı & Dirmenci (CS), *Cirsium trachylepis* Boiss. (CT)

were collected from Elazığ (1125 m, 11.08.2017), Antalya (1200 m, 18.08.2017), Çanakkale (50–100 m, 05.09.2017), Eskişehir (930 m, 15.09.2017), Sivas (1706 m, 05.08.2017), Trabzon (1785 m, 11.08.2016), respectively. The voucher specimens were deposited at the Herbarium of Faculty of Education, Balikesir University (Balıkesir, Turkey) and Faculty of Pharmacy, Ankara University with voucher numbers "Dirmenci 4913 & Arabacı", "Dirmenci 4953", "Dirmenci 4935", "Dirmenci 4946", "Dirmenci 4824 & Arabacı" and "AEF 27191", respectively. The species were identified by Prof. Dr. Tuncay DIRMENCI, Prof. Dr. Turan ARABACI, and Prof. Dr. Ufuk ÖZGEN.

Bio-activity-guided fractionation studies with collagenase inhibition

Preparation of extract

Air-dried and finely powdered aerial parts and roots were extracted with CH_3OH three times, taking 8 h at room temperature for each extraction. The combined extracts were evaporated under reduced pressure at 40 °C to obtain crude extracts. The crude methanol extracts of CA, CD, CE, CP, CS, and CT were applied to bio-activity-guided fractionation studies guided by in vitro collagenase inhibition studies (Şener et al. 2021). The methanol extract yield % of aerial parts of CA (CAA), CD (CDA), CE (CEA), CP (CPA), CS (CSA), and CT (CTA) were found as 5.25%, 6.32%, 5.85%, 4.78%, 4.95% and 6.56%, respectively. The methanol extract yield% of roots of CA (CAR), CD (CDR), CE (CER), CP (CPR), CS (CSR), and CT (CTR) were evaluated as 6.13%, 7.25%, 5.25%, 5.95%, 6.25% and 7.35%, respectively.

Collagenase inhibition assay

Methanol extracts of all *Cirsium* species, also subfractions, and other fractions of the most effective *Cirsium* genus were investigated for collagenase inhibition with the modified method using FALGPA as substrate (Akkol et al. 2015; Thring et al. 2009; Singh et al. 1996). All dry fractions were dissolved into the buffer solution (0.2 M Tris–HCl buffer, pH 7.8) in the different concentration ranges of 25–400 µg/mL. In positive control, EGCG was dissolved in the range of 6.25–100 µg/mL. The test procedure was designed as A, B, C, and D wells, described as A, 25 µL enzyme solution (0.8 units/mL), 50 µL substrate solution (2 mM FALGPA in buffer solution); 50 µL buffer solution (0.1 M Tris–HCl buffer, pH 8.0), B; 25 µL enzyme solution, 100 µL buffer solution, C; 25 µL enzyme, 50 µL substrate solution, 25 µL sample solution, 25 µL buffer solution, D; 25 µL enzyme solution, 25 µL sample solution, 75 µL buffer solution. After that, the plates were incubated at room temperature for 15 min. Following the incubation, the substrate solution was mixed into the corresponding well. The plates were incubated for 15 min, again. The absorbances of the reaction mixtures were specified spectrophotometrically at 340 nm using a spectrophotometer (SpetrostarNano BMG LABTECH). Each sample was run three times to control the repeatability of the assay. The percentage of collagenase inhibitory effect was estimated with the specified equation:

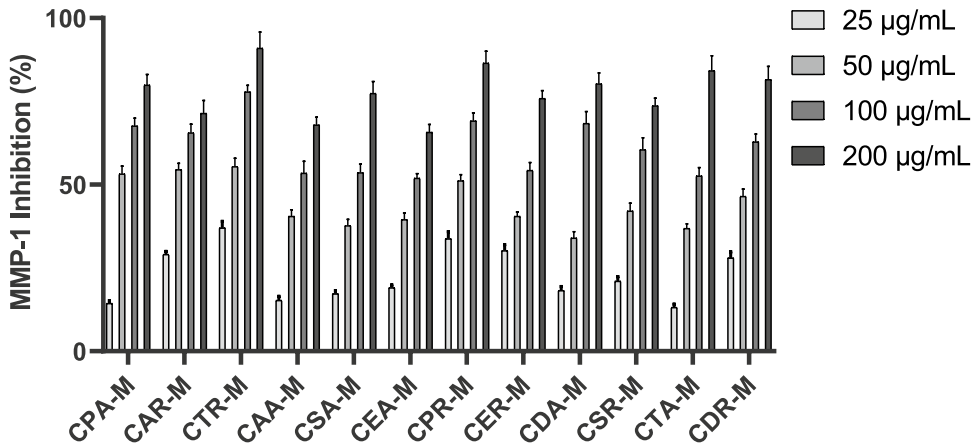

Fig. 1 The graph of percentage MMP-1 inhibition of effective samples (CAR-M: Methanol extract of *C. aristatum* root, CAA-M: Methanol extract of *C. aristatum* aerial parts, CDR-M: Methanol extract of *C. dirmilense* root, CDA-M: Methanol extract of *C. dirmilense* aerial parts, CER-M: Methanol extract of *C. elodes* root, CEA-M: Methanol extract of *C. elodes* aerial parts, CPR-M: Methanol extract of *C. pseudocreticum* root, CPA-M: Methanol extract of *C. pseudocreticum* aerial parts, CSR-M: Methanol extract of *C. sivasicum* root, CSA-M: Methanol extract of *C. sivasicum* aerial parts, CTR-M: Methanol extract of *C. trachylepis* root, CTA-M: Methanol extract of *C. trachylepis* aerial parts, CTR-A: Aqueous subfraction of *C. trachylepis* root, CTR-E: EtOAc subfraction of *C. trachylepis* root, Se: Sephadex, Fr: Fraction)

$$\text{Collagenase Inhibition (\%)} = ((A - B) - (C - D))/(A - B) \times 100$$

Afterward, a graph was used to estimate the values of the half-maximal inhibitory concentration (IC_{50}) for collagenase.

Bio-activity-guided fractionation studies for CT

CTR was determined for proceeding with bio-activity-guided fractionation concerning collagenase inhibition studies (Fig. 1). To prepare subfractions, the methanol extract of CT (25 g) was suspended in 300 mL of H_2O: CH_3OH (9:1). It was partitioned against chloroform ($CHCl_3$) (300 mL × 3) and ethyl acetate (EtOAc) (300 mL × 3), respectively. The chlorofrom EtOAc subfractions were evaporated at reduced pressure at 40 °C, and were 12.00 g and 600 mg, respectively. The aqueous phase was evaporated to give a residue (11.00 g). Based on collagenase inhibition, the EtOAc fraction was chosen to proceed with bio-activity-guided fractionation studies. The EtOAc fraction was subjected to a Sephadex column using isocratic elution with 100% CH_3OH, and 19 fractions were obtained. Elutioned fractions were subjected to thin layer chromatography (TLC) with a solvent system of EtOAc:CH_3OH:H_2O (v/v/v, 7:2:1). Similar fractions were assembled. The combined 7 fractions were evaluated for collagenase inhibition, and the most active fraction was specified as 16–17 fractions (CTR-E1, 1,5-dicaffeoylquinic acid, 40 mg) compared with other combined fractions (Fig. 2).

Isolation studies were continued on the chloroform and remaining aqueous subfraction. Silica gel column chromatography was applied to the chloroform subfraction of the roots, and gradient elution was performed in the *n*-hexane:EtOAc (100:0–0:100) solvent system. A total of 54 subfractions were collected. Subfractions 28-29 were combined according to TLC analysis (*n*-hexane:EtOAc (8:2)) and subjected to semi-preparative HPLC. For the semi-preparative HPLC method, a semi-preparative HPLC column (Zorbax® C18, 9.4 × 250 mm, 5 µM particle size, Part No. 880952-202), a flow rate of 1.5 mL/min, an injection volume of 100 µL with a diode array detector at 210 nm and 240 nm. The gradient elution conditions 0–49.00 min → 20% H_2O, 80% MeCN; 49.01–59.00. min → 6% H_2O, 94% MeCN; 59.01–60.00 min → 0% H_2O, 100% MeCN were applied.

Upon examination of the HPLC chromatogram, it was decided to collect fractions of the mixture at specific minutes (5–15 min; 15–30 min; 30–45 min; and 45–60 min) (Supplementary material 1). After collection at specified minutes, the fractions were subjected to ^{1}H-NMR and

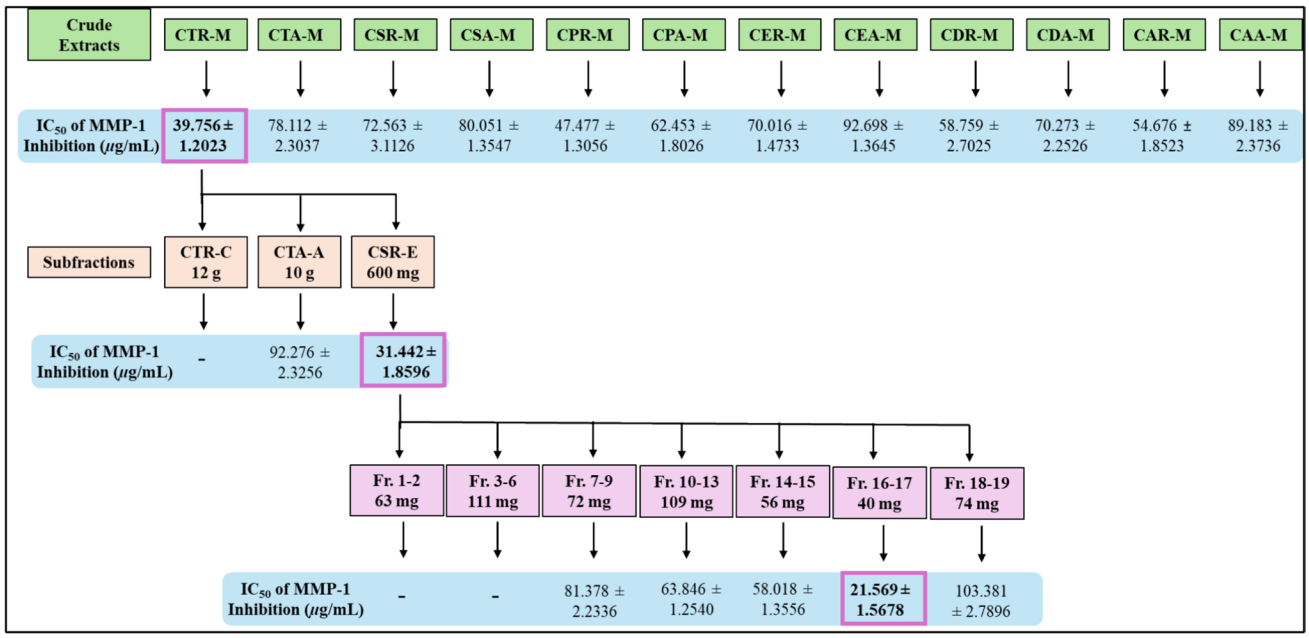

Fig. 2 Shematic diagram of bio-activity guided fractionation studies (CAR-M: Methanol extract of *C. aristatum* root, CAA-M: Methanol extract of *C. aristatum* aerial parts, CDR-M: Methanol extract of *C. dirmilense* root, CDA-M: Methanol extract of *C. dirmilense* aerial parts, CER-M: Methanolic extract of *C. elodes* root, CEA-M: Methanol extract of *C. elodes* aerial parts, CPR-M: Methanolic extract of *C. pseudocreticum* root, CPA-M: Methanol extract of *C. pseudocreticum* aerial parts, CSR-M: Methanol extract of *C. sivasicum* root, CSA-M: Methanol extract of *C. sivasicum* aerial parts, CTR-M: Methanol extract of *C. trachylepis* root, CTA-M: Methanol extract of *C. trachylepis* aerial parts,, CTR-A: Aqueous subfraction of *C. trachylepis* root, CTR-E: EtOAc subfraction of *C. trachylepis* root, Se: Sephadex, Fr: Fraction)

^{13}C-NMR spectroscopic analyses. It was determined that the fraction collected at 5–15 min contained Lupeol, while the other fractions were found to be in a mixed state. The compound collected at 5–15 min, designated as CTR-C1, was re-chromatographed using the HPLC method, and its purity was also tested by the HPLC method (Supplementary material 2).

An octadecyl phase (C18) column was applied to the remaining water subfraction. Chromatographic analysis was carried out using a gradient elution system (H_2O:CH_3OH 99:1 → 0:100). The fractions obtained were subjected to TLC analysis (EtOAc:CH_3OH:H_2O (7:2:1)), and fractions 35–40 were combined and applied to a Sephadex column. The 7th subfraction out of the 12 subfractions obtained by the Sephadex column with a 100% methanol elution system was purified, and given the code CTR-A1 (tryptophan, 9.6 mg).

Structure elucidation of the isolated compounds

The structural elucidation of CTR-E1 was achieved through the utilization of NMR data obtained from a Bruker Ascend Instrument operating at 400 MHz (^{1}H-NMR) and 100 MHz (^{13}C-NMR), alongside mass spectral analyses conducted with a Waters Micromass® ZQ™ Mass Spectrometer. The findings were ultimately checked by comparing the results with previously published data. The compound CTR-E1 was identified as 1,5-dicaffeoylquinic acid, while CTR-C1 was determined to be lupeol, and CTR-A1 was recognized as tryptophan.

LC–MS/MS analysis

Preparation of sample solution

0.75 mL of CTR-M (3 mg) and CTA-M (3 mg) were dissolved in EtOH:H_2O (60:40 v/v) and then were refluxed in EtOH: H_2O (60:50 v/v) for 1 h. Subsequently, 400 µL of this solution was transferred into the volumetric vial. Then, 50 µL of curcumin (Internal Standard) was added and diluted with 500 µL of mobile phase. 10 µL of the prepared sample solution was injected into LC.

Instruments and chromatographic conditions

Qualitative and quantitative analysis of 13 secondary metabolites in extracts was performed by the developed LC–MS/MS method (Gülçin et al. 2020; Kiziltas et al. 2022; Seyhan et al. 2019). LC–MS/MS analysis was conducted using a Zivak® HPLC and Zivak® Tandem Gold Triple quadrupole mass spectrometry equipped with a Synergy Max C18 column (250 × 2 mm i.d., 5 µm particle size) and gradient program with a two solvent system A: 0.1% formic acid in deionized water; B: 0.1% formic acid in CH_3OH at a constant solvent flow rate of 0.25 mL/min with a diode array detector at 280 nm, and the column temperature was set to 30 °C. The gradient program was as follows: 0–1.00 min 55% A, 45% B; 1.01–20.00 min 0% A, 100% B; 20.01–25.00 min 55% A, 45% B.

Optimization of HPLC methods and LC–MS/MS procedure

The optimal mobile phase was identified as a gradient system comprising acidified methanol and water. This mobile phase proved effective for enhancing the ionization efficiency and separation of the target compounds. The electrospray ionization (ESI) source facilitated the effective ionization of small, relatively polar antioxidants. In quantitative mass spectrometry analyses, the ionization technique and collision energies are critical parameters. The triple quadrupole mass spectrometry system is frequently employed due to its ability to maintain stable fragmented ions. Consequently, the decision was made to utilize this system. The ideal ESI parameters were established as follows: 2.40 mTorr for CID gas pressure, 5000.00 V for ESI needle voltage, 600.00 V for ESI shield voltage, 300.00 °C for drying gas temperature, 50.00 °C for API housing temperature, 55 psi for nebulizer gas pressure, and 40.00 psi for drying gas pressure.

Validation of experiments and uncertainty evaluation

The LC–MS/MS method validation parameters were used as linearity, repeatability, the limit of detection (LOD), and limit of quantification (LOQ) trials (Gülçin et al. 2020; Kiziltas et al. 2022; Seyhan et al. 2019). The evaluation of sources and quantification of uncertainty in the LC–MS/MS method was conducted using the EURACHEM/CITAC guide (EURACHEM/CITAC Guide CG 4 2012). The validation and uncertainty parameters for the 13 compounds were presented in this study. The linearity of additional compounds in the described method was established through the examination of standard solutions. The ranges of linearity for each compound are detailed in Table 1. The correlation coefficients (r^2) were determined to be equal to or greater than 0.98. Additionally, the linear regression equations for the compounds under investigation are provided in Table 1, where y represents the peak area and x denotes the concentration. The limits of detection (LOD) and limits of quantification (LOQ) for the LC–MS/MS methodologies applied to the compounds were established to range from 0.5 to 50 mg/L. The LODs were defined as three times the standard deviation, whereas the LOQs were set at ten times the standard deviation. The intra-day repeatability was expressed as recovery % which were derived from the peak area measurements of three replicate analyses. The concentration of each analyte within the linear range, as well as

Table 1 Validation and uncertainty parameters

	Compounds	Linear regression equation	R^2	LOD/LOQ	Recovery (%)
1	1,5-dicaffeoylquinic acid	y = 0.013x − 0.002	0.9983	0.02/0.07	93.49
2	Chlorogenic acid	y = 0.300x − 0.039	0.9980	0.45/1.49	94.55
3	(-)-Epicatechin	y = 0.029x − 0.001	0.9963	0.02/0.06	96.38
4	Epigallocatechin gallate	y = 0.118x − 0.010	0.9957	0.10/0.32	95.21
5	Fumaric acid	y = 0.060x + 0.020	0.9940	0.06/0.22	94.56
6	Gallic acid	y = 0.039x − 0.016	0.9985	0.54/1.79	92.77
7	Kaempferol	y = 0.002x + 0.009	0.9937	0.02/0.08	94.55
8	Luteolin	y = 0.219x + 0.035	0.9964	0.65/2.15	98.41
9	Luteolin-5-O-glucoside	y = 0.225x + 0.037	0.9930	0.04/0.14	98.88
10	Luteolin-7-O-glucoside	y = 0.135x + 0.019	0.9973	0.20/0.68	91.44
11	Pelargonin chloride	y = 0.189x + 0.004	0.9928	0.17/0.57	95.55
12	Pyrogallol	y = 0.040x + 0.015	0.9880	0.04/0.16	94.53
13	Quercetin	y = 0.120x + 0.030	0.9911	0.31/1.03	98.86

the concentration associated with the reported method, was derived from the calibration curve. The validation parameters and uncertainty parameters of other compounds have been presented in Table 1.

In vitro cytotoxic activity on SK-Mel

The MTT assay was used to evaluate the cytotoxic activity of SK-Mel and NHDF cells. The bio-activity-guided fractionation studies' most effective species, CT, was selected to uncover cytotoxic activity against SK-Mel. The cytotoxic effects of methanol extract and subfractions of CT were tested (Badem et al. 2021). SK-Mel cells were maintained in alpha-MEM containing 10% FBS, gentamicin, and amphotericin, and incubated for 24 h at 37 °C and 5% CO_2 atmosphere. Toxic effects on normal human cells were tested using NHDF cells. NHDF cells were cultured in alpha-MEM containing 10% FBS, gentamicin, and amphotericin. Cisplatin was used as a positive control and samples were added to evaluate cytotoxic effects on related wells at different concentration ranges (0.09–200 µg/mL). Cells were incubated at 37 °C and 5% CO_2 atmosphere for 48 h. MTT solution (5 mg/mL) was added to each well. The cells were incubated at 37 °C and 5% atmosphere for 2 h. Then, dimethyl sulfoxide was added to dissolve the formazan crystals in the wells and incubated for 30 min. The absorbances were measured with an ELISA microplate reader at a wavelength of 570–620 nm. The toxic effect of the samples on the cells was found using the following formula:

$$\%\ \text{Vitality} = (\text{The optical density of the sample})/(\text{The optical density of the control}) \times 100$$

The IC_{50} values of samples were calculated using the non-linear dose–response curve using the GraphPad software program. The selective toxic effect of the samples on cancer cells (SI = normal cell toxic effect/cancer cell toxic effect) was determined by comparing the toxicity of the samples for HFC.

In silico analysis

Molecular docking is a computational method that predicts the binding mode and affinity of a small molecule (ligand) to a macromolecule (protein). It involves generating a 3D model of both the ligand and protein and then predicting their ideal orientation and interaction energy. By simulating the binding process, researchers can predict the likelihood of a given ligand binding to a particular protein target and can use this information to design new drugs or optimize existing ones (Khan et al. 2016). The 3D structures of the test compound CTR-E1 (CID6474640), as well as the reference compound, EGCG were downloaded from the PubChem Database (https://pubchem.ncbi.nlm.nih.gov/) for molecular docking studies with the chosen enzyme (receptors) (Kim et al. 2023). The RCSB Protein Database (https://www.rcsb.org/pdb) was used to download the 3D structures of the receptor collagenase (PDB ID 2Y6I) (Berman et al. 2000). CASTp (http://sts.bioe.uic.edu/castp/index.html?2r7g) server was used to predict the active site of enzymes (Tian et al. 2018). This particular crystal structure was removed from water and ion molecules. Additionally, the APBS-PDB2PQR tool (https://server.poissonboltzmann.org/pdb2pqr) was used to structure the missing hydrogen atoms and atomic charges (Jurrus et al. 2018). The BIOVIA Discovery Studio 2020 Client application was used to convert the 3D structures of these compounds to.pdb format (Dassault 2020). The target proteins and ligands' structures

were prepared, and AutoDock 4.2 was used to perform molecular docking with the Lamanckian genetic algorithm (Morris et al. 2009). All molecules were analyzed through molecular docking at the predicted active site of the model enzyme. The docking data described the binding interaction (hydrogen/hydrophobic) and affinity indicated by the docking score of the ligand on the target protein. The top model for each receptor-ligand interaction as well as the binding results table was kept for visualization. Once the docking is complete, the binding results are analyzed, and the protein–ligand interactions are visualized using software such as BIOVIA Discovery Studio Visualizer (Dassault 2020). This allows for a more detailed understanding of the binding model and potential interactions that may be exploited for drug design.

Results and discussion

Nowadays, skin cancer is a growing health challenge that causes health problems and economic costs. Melanoma which constitutes 1% of skin cancer, is the most metastasizing skin cancer type and has a 15–20% five-year survival rate (Khan et al. 2021). It was clinically demonstrated that interstitial collagenase, MMP-1 enhances the malignancy of melanoma cells. Therefore, interstitial collagenase, MMP-1 inhibitors can be a beneficial approach for the treatment of melanoma due to their ability to retard the metastasis of melanoma cells (Lida and McCarthy 2007; Kerkelä et al. 2003). Natural sources are among the favorite sources for the pharmaceutical industry to discover new drugs due to their obtainability and lower side effects compared with synthetic drugs for melanoma therapy (Chinembiri et al. 2014). *Cirsium* genus is represented by 68 species (80 taxa, 33 endemics) in Turkey (Duman et al. 2017; Dirmenci et al. 2020).

Some *Cirsium* species have been reported to have therapeutic potential for melanoma owing to the decreasing effect of interstitial collagenase, and MMP-1 expression (Nazaruk et al. 2014; Sim et al. 2007; Yoon et al. 2022). This information led us to investigate the therapeutic effect of other *Cirsium* species on melanoma through collagenase inhibition.

Results of bio-activity guided fractionation studies guidance with collagenase inhibition

In vitro collagenase inhibition studies on the aerial parts and roots of six *Cirsium* species showed that the most effective extract belonged to the roots of CT ($IC_{50} = 39.756 \pm 1.2023$ µg/mL) (Fig. 1). Therefore, bio-activity-guided fractionation studies were maintained for the roots of CT. The most effective subfraction from the roots of CT was observed as EtOAc ($IC_{50} = 31.442 \pm 1.8596$ µg/mL) to continue the bio-activity guided isolation study. It was evaluated that CTR-E-Se Fr-16-17 obtained from EtOAc subfraction by Sephadex column had the highest collagenase inhibition (Fig. 2).

Bio-activity-guided fractionation studies led to the purification of 1,5-dicaffeoylquinic acid called CTR-E1 obtained from the EtOAc subfraction of CT's root (Fig. 3, Supplementary Materials 3). Additional isolation studies were also performed on other sub-fractions ($CHCl_3$ and n-BuOH) of CTR. 2 different compounds (CTR-C1 and CTR-B1) were obtained from these fractions (Supplementary Materials 4–10).

CTR-E1 indicated $[M\text{-}H]^+$ ion at m/z 515.09 ($C_{25}H_{24}O_{12}$). ^{1}H-NMR (CD_3OD, 400 MHz): δ 7.59 (d, $J = 15.9$ Hz, H-7′, H-7″), 7.07 (s, H-2′, H-2″), 6.97 (dd, $J_1 = 2.2$ Hz, $J_2 = 2.2$ Hz, H-6′, H-6″), 6.80 (d, $J = 8.2$ Hz, H-5′, H-5″), 6.34 (d, $J = 12.7$ Hz, H-8′), 6.30 (d, $J = 12.7$ Hz, H-8″), 5.42 (td, $J_1 = 9.2$ Hz, $J_2 = 9.2$ Hz, $J_2 = 3.8$ Hz, H-5), 4.28 (dd, $J_1 = 7.6$ Hz, $J_2 = 3.7$ Hz, H-3), 3.77 (dd, $J_1 = 8.7$ Hz, $J_2 = 3.3$ Hz, H-4), 2.60 (m, H-2b, H-6b), 2.36 (dd, $J_1 = 14.8$ Hz, $J_2 = 3.4$ Hz, H-2a), 2.05 (dd, $J_1 = 13.4$ Hz, $J_2 = 9.9$ Hz, H-6a); ^{13}C—NMR (CD_3OD, 100 MHz): δ 175.0 (C7), 167.5 (C-9′), 148.2 (C-4′), 148.1 (C-4″), 145.7 (C-7′), 145.6 (C-7″), 145.4 (C-3′), 145.3 (C-3″), 126.5 (C-1′), 126.4 (C-1″), 121.6 (C-6′, C-6″), 115.5 (C-5′, C-5″), 114.5 (C-2′), 114.0 (C-2″), 113.8 (C-8′), 113.8 (C-8″), 81.0 (C-1), 72.2 (C-4), 70.2 (C-5), 68.7 (C-3), 36.2 (C-6), 34.8 (C-2). ^{1}H-NMR analysis of CTR-E1 verified signals for the moieties of two caffeic acids and a quinic acid (Fig. 3). Three different aromatic proton signals at 6.80–7.07 ppm indicated the possible presence of 1,3,4-trisubstituted benzenes. For the first caffeic acid moiety, two doublet signals at 7.59 and 6.34 ppm with the large 15.9 Hz splitting typical for olefinic proton trans-configurations were attributed to H-7′ and H-8′. The previous doublet signals at 7.59 ppm, overlapping and integrated for 2H, were assigned to H-7″ in addition to H-7′. Another doublet signal at 6.31 ppm with a large splitting of 15.9 Hz belonged to H-8″ of the second caffeic acid moiety. The overlapping and integrated 2H singlet signal at 7.07 ppm was assigned to H-2′ and H-2″. The signal of H-5 belonging to the caffeoyl moiety was detected more downfield (5.42 ppm) than the signals of H-3 (4.28 ppm) and H-4 (3.77 ppm) of the quinic acid skeleton, suggesting that the second caffeoyl moiety was bonded to the C-1 position of the quinic acid skeleton (Tolonen et al. 2002). Overlapping signals observed at 2.60 ppm and integrated for 2H were also attributed to aliphatic methylene protons of H-2b and H-6b. We attributed the two doublet signals at 2.36 and 2.05 ppm to the

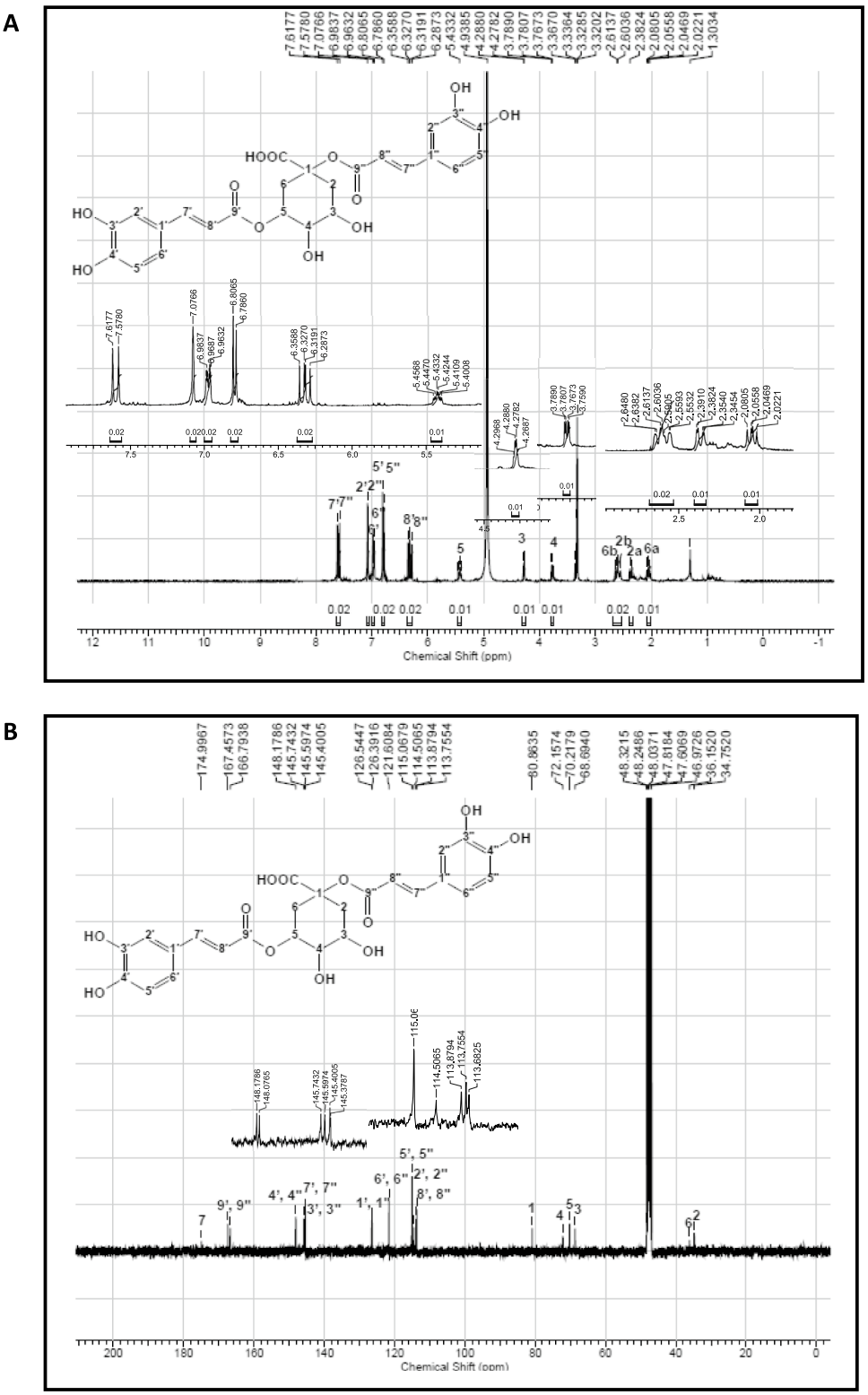

Fig. 3 ^{1}H-NMR spectrum (CD_3OD, 400 MHz) **A** and ^{13}C-NMR spectrum (CD_3OD, 100 MHz) **B** of CTR-E1 (1,5-dicaffeoylquinic acid)

other methylene protons, H-2a and H-6a, respectively. The structure of 1,5-dicaffeoylquinic acid for CTR-E1 was also verified by analysis of ^{13}C-NMR data, MS analysis, and comparison with literature data (Kim et al. 2005; Tolonen et al. 2002; Etemadi-Tajbakhsh et al. 2020; Zheng et al. 2018).

CTR-C1 was displayed m/z: 425.51 $[M-H]^+$ ($C_{30}H_{50}O$) ion according to MS analysis. ^{1}H-NMR ($CDCl_3$, 400 MHz): δ 4.70 (bs, H-29b), 4.60 (bs, H-29a), 3.21 (dd, $J_1 = 11.2$ Hz,

$J_2 = 4.8$ Hz, H-3), 2.40 (sextet, $J_1 = 10.9$ Hz, $J_2 = 5.8$ Hz, H-19), 1.94 (m, H-21a), 0.67–1.69 (m, H-1, H-2, H-5, H-6, H-7, H-9, H-11, H-12, H-13, H-15, H-16, H-18, H-22), 1.69 (s, H-30), 1.37 (m, H-21b), 1.04 (s, H-26), 0.98 (s, H-23), 0.96 (s, H-27), 0.85 (s,H-25), 0.80 (s, H-28), 0.77 (s, H-24); ^{13}C-NMR ($CDCl_3$, 100 MHz): δ 151.0 (C-20), 109.4 (C-29), 79.0 (C-3), 55.3 (C-5), 50.4 (C-9), 48.2 (C-18), 48.0 (C-19), 43.0 (C-17), 42.8 (C-14), 40.1 (C-8), 40.0 (C-22), 38.9 (C-4), 38.7 (C-1), 38.0 (C-13), 37.1 (C-10), 35.6 (C-16), 34.3 (C-7), 29.7 (C-21), 28.0 (C-23), 27.4 (C-2), 27.4 (C-15), 25.1 (C-12), 20.9 (C-11), 19.3 (C-30), 18.3 (C-6), 18.0 (C-28), 16.1 (C-25), 16.0 (C-26), 15.4 (C-24), 14.6 (C-27). The sextet signal at 2.40 ppm corresponding to 19β-H is a defining feature of lupeol. The doublet of doublets at 3.21 ppm was assigned to H-3. Two singlets at 4.60 ppm and 4.70 ppm were attributed to olefinic protons of H-29a, and H-29b. ^{13}C NMR experiments revealed seven methyl groups at 28.0 ppm, (C-23); 18.0 ppm, (C-28); 16.1 ppm, (C-25); 16.0 ppm, (C-26); 15.4 ppm, (C24); 14.6 ppm, (C-27); 19.3 ppm, (C-30). The signals belonging to the exo-methylene group at 109.4 ppm (C-29) and 151.0 ppm (C-20) were evidenced lupeol structure. The signal at 79.0 ppm was attributed to C-3 which was bonded to a hydroxyl group. The compound was confirmed as lupeol in comparison to previous articles (Silva et al. 2017).

CTR-B1 was displayed m/z: 202.91 $[M-H]^+$ ($C_{11}H_{12}N_2O_2$) ion according to MS analysis. ^{1}H-NMR (CD_3OD, 400 MHz): δ 7.72 (d, $J = 7.8$ Hz, H-5), 7.38 (d, $J = 8.1$ Hz, H-8), 7.21 (s, H-4), 7.13 (t, $J = 8.0$ Hz, H-5), 7.06 (t, $J = 8.0$ Hz,, H-6), 3.91 (m, H-10), 3.53 (dd, $J = 14.8$, 4.0 Hz, H-11b), 3.17 (dd, $J = 15.1$, 9.4 Hz, H-11a). ^{13}C-NMR (CD_3OD, 100 MHz): δ 173.0 (C-1), 137.0 (C-2), 127.1 (C-3), 123.5 (C-4), 121.3 (C-5), 118.7 (C-6), 117.9 (C-7), 111.0 (C-8), 108.1 (C-9), 55.3 (C-10), 27.0 (C-11). Tryptophan displays a distinctive characteristic with peaks at 3.53 and 3.17 ppm, corresponding to H-11a and 11-b respectively. The singlet peak for H-4 was detected at 7.21 ppm. A single methylene group was pinpointed through ^{13}C NMR analysis at 27.0 ppm (C-11). Another carbon signal at 55.3 ppm was linked to C-10. The C-1 carbonyl signal was observed at 173.0 ppm. Furthermore, the other C signals were consistent with tryptophan based on findings from previous literature studies (Huaxi et al. 2020; Malta et al. 2009; Domingues et al. 2003).

Results of LC–MS/MS analysis

We detected and quantified a total of 13 secondary metabolites in CTR-M and CTA-M based on LC–MS/MS analysis. The available compounds in CTR-M were 1,5-dicaffeoylquinic acid (55.26 mg/g), epicatechin (33.91 mg/g), fumaric acid (59.87 mg/g), and pyrogallol (53.02 mg/kg). Chlorogenic acid (63.59 mg/g) and luteolin-7-O-glucoside (35.10 mg/g) were detected in CTA-M. Comprehensive details regarding the experimental parameters and the amounts of compounds in CTR-M and CTR-A are presented in Table 2, Supplementary Materials 11.

Although studies on the inhibitory effect of CTR-E1 on collagenase have not been found, there are some studies about the effect on collagenase for other dicaffeoyl quinic acid derivatives. 3,5-dicaffeoyl quinic acid application on UVA-irradiated HDFs has been proven to downregulate interstitial collagenase, MMP-1 expression by blocking the MAPK-cascade (Oh et al. 2020). 1,5-dicaffeoyl quinic acid named as CTR-E1 has been shown to possess (61%)

Table 2 LC–MS/MS parameters of selected compounds and the amounts of phenolic compounds in mg/g crude extracts

	Compounds	ESI mode	Parent ion	Daughter ion	Collision energy (V)	CTR-M (mg/g crude extract)	CTA-M
1	1,5-dicaffeoylquinic acid	Neg	515.0	353.0	16	55.26 ± 4.02	–
2	Chlorogenic acid	Neg	353.0	191.0	14	–	63.59 ± 8.98
3	Epicatechin	Neg	289.0	245.0	14	33.91 ± 2.69	–
4	Epigallocatechin gallate	Neg	457.0	169.0	14	–	
5	Fumaric acid	Neg	115.0	71.0	8	59.87 ± 5.55	–
6	Gallic acid	Neg	168.6	124.0	13		
7	Kaempferol	Pos	287.0	152.3	30	–	–
8	Luteolin	Neg	285.0	132.0	34		–
9	Luteolin-5-O-Glucoside	Neg	447.0	289.5	20	–	–
10	Luteolin-7-O-Glucoside	Neg	447.0	284.5	22	–	35.1 ± 2.44
11	Pelargonin chloride	Pos	595.0	271.0	30	–	–
12	Pyrogallol	Neg	125.0	80.0	16	53.02 ± 6.52	–
13	Quercetin	Neg	301.0	178.5	16	–	–

– Not detected, *Neg* negative, *Pos* positive

Table 3 IC_{50} values (µg/mL) and selectivity index calculated for methanol extract and subfractions of CTR and cisplatin on SK-MEL and NHDF cells (n = 3)

Test compounds	NHDF	SK-MEL	Selectivity index
CTR-M	122.8	129.4	0.95
CTR-C	123.8	134.7	0.92
CTR-A	178.3	133.3	1.34
CTR-E	129.3	119.4	1.08
Cisplatin	5.2	3.22	1.61

CTR-M methanol extract of *C. trachylepis* root, *CTR-C* chloroform subfraction of *C. trachylepis* root, *CTR-A* aqueous subfraction of *C. trachylepis* root, *CTR-E* EtOAc subfraction of *C. trachylepis* root

anti-melanogenesis effect which is a greater rate than positive control arbutin (35%) (Ha and Park 2018).

Epicatechin has been proven to possess the therapeutic effect on UV-induced human skin fibroblast cells by enhancement of gene expression levels of Collagen I Alpha 1, fibroblast growth factor-2, and glutathione peroxidase-1, while simultaneously leading to a reduction in the gene expression of MMP-1 (Widowati et al. 2024). Fumaric acid, and pyrogallol-detected compounds by LC–MS/MS analysis have not been reported to have direct collagenase inhibition effects in the available studies. Although each of these compounds is known to be effective for some dermalogical diseases like psoriasis, there is a lack of specific research investigating their roles as collagenase inhibitors

Table 4 Molecular docking results of 1,5-dicaffeoylquinic acid and reference molecules against Collagenase G

Enzyme name	PDB ID	Compound name	Binding energy (kcal/mol)	K_i	Number of H-bonds interactions	Residues interacting with the compound
Collagenase G	2Y6I (Chain A) Res: 3.25 Å	CTR-E1	− 8.19	987.87 nM	4	Glu524, Glu498, Pro499, Ile497, Trp539, Gly494, Tyr496
		*EGCG	− 6.98	7.59 µM	7	His523, Glu524, Glu559, Tyr496, Leu495, Asp491, Gly493

*Reference compound, *CTR-E1* 1,5-dicaffeoylquinic acid, *EGCG* epigallocatechin gallate

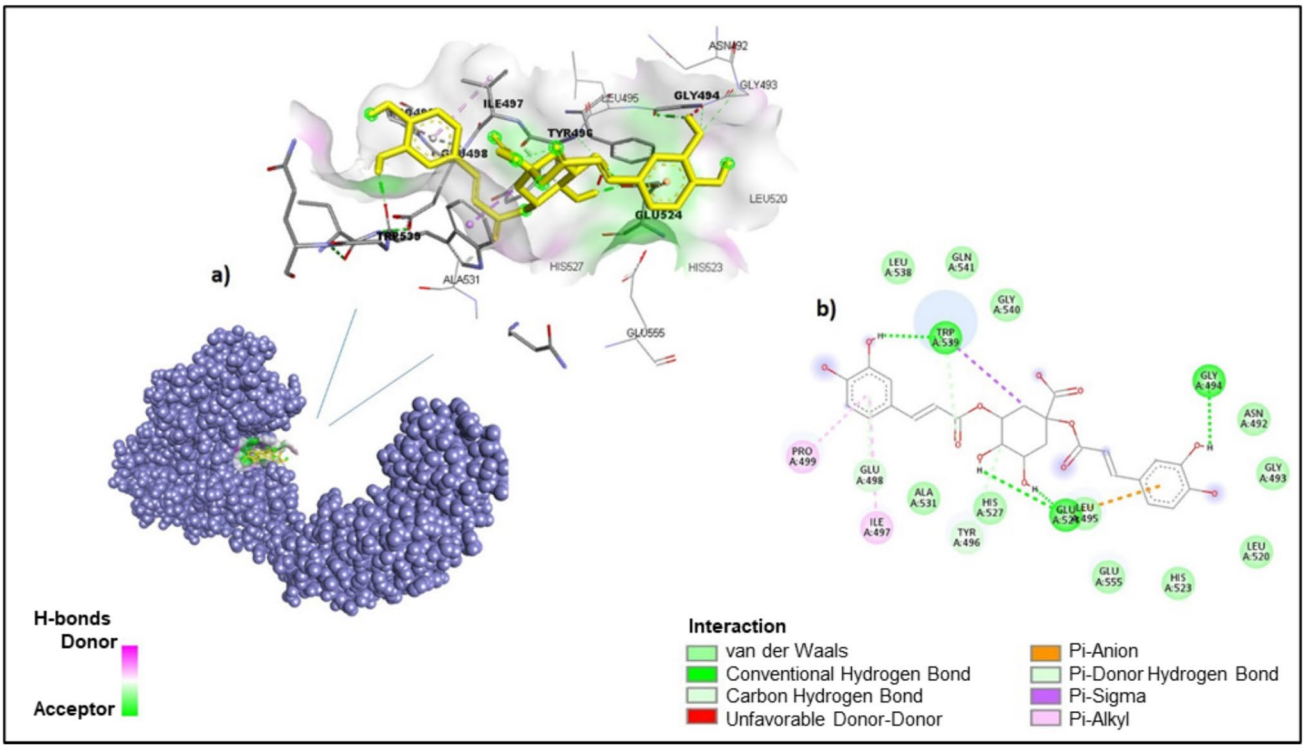

Fig. 4 Collagenase-1,5-dicaffeoylquinic acid docking poses. **a** Three-dimension (3D) and **b** the two-dimension (2D) interaction analysis of collagenase with 1,5-dicaffeoylquinic acid (CTR-E1)

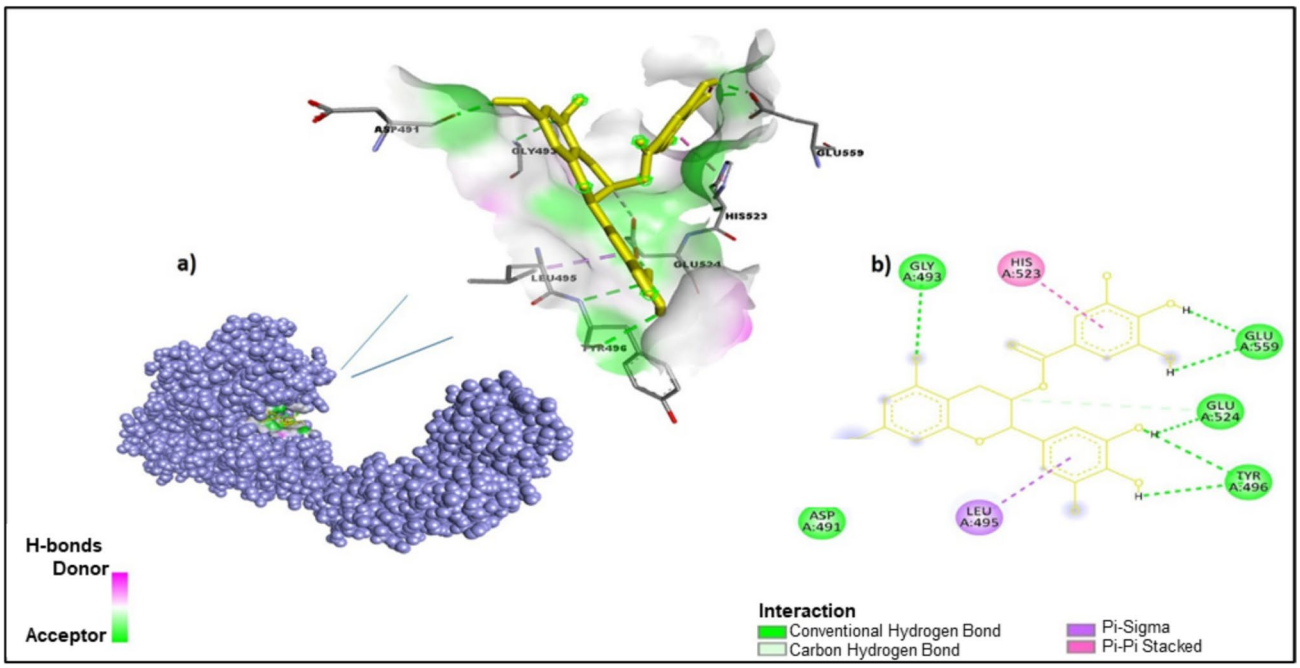

Fig. 5 Collagenase-EGCG docking poses. **a** Three-dimension (3D) and **b** the two-dimension (2D) interaction analysis of collagenase with EGCG

(Smith, 2017; Upadhyay et al. 2010). Further studies are needed to explore their potential in this regard.

Results of in vitro cytotoxic activity studies on SK-Mel

The anticancer effects of the methanol extract and subfractions of the CT roots were evaluated on SK-Mel. The CTR-M and CTR-E demonstrated significant efficacy in exhibiting anticancer properties.

The highest anticancer effect was observed for the EtOAc subfraction ((IC_{50} = 119.4 ± 2.5023 µg/mL), SI:1.08) (Table 3). It was proven that 25 µM of 1,5-dicaffeoylquinic acid decreased the proliferation of B16F1 murine melanoma cells induced by melanocyte-stimulating hormone (α-MSH) by 26% and 61%, respectively (Ha and Park 2018). The potential anticancer effect of the EtOAc subfraction of CT may be related to its collagenase inhibitory effect and 1,5-dicaffeoylquinic acid content.

The methanol extract of the species has also been found to exhibit anticancer activity in melanoma cells ((IC_{50} = 129.4 ± 3.3525 µg/mL), SI:0.95) (Table 3). Research has not identified any studies specifically examining the direct efficacy of fumaric acid in the treatment of melanoma. However, it has been established that the fumaric acid ester dimethyl fumarate demonstrates effectiveness against metastatic melanoma cells, primarily through its inhibitory action on NF-kB (Loewe et al. 2006). It was proven that chlorogenic acid inhibited the proliferation of melanoma C32 cells by enhancing the expression of antioxidant molecules, including superoxide dismutase and glutathione peroxidase, which leads to a reduction in oxidative stress. Additionally, chlorogenic acid impedes the growth of B16F10 melanoma cells by promoting the polarization of tumor-associated macrophages from the M2 phenotype to the M1 phenotype (Nguyen et al. 2024). Research has demonstrated that Luteolin-7-O-glucoside at concentrations of 50, 100, and 200 µM significantly decreased both melanin synthesis and tyrosinase activity in B16F10 mouse melanoma cells (Choi et al. 2022). The anticancer effectiveness of CTR-M may be linked to additional compounds, including chlorogenic acid and luteolin-7-O-glucoside, which were identified through LC–MS/MS analysis.

Results of in silico analysis

To research potential drugs, several computer-based techniques are available, such as molecular docking and molecular dynamics simulations. The primary purpose of molecular docking is to examine the numerous binding interactions that potential medications might have with specific locations or active sites on target molecules. The binding efficacy of a ligand molecule with a target has been widely described

by analyzing the hydrogen bonding pattern and the type of residues present in the active site, among all the other types of interactions such as H-bond, π–π, and amide − π interactions. The binding affinity of various ligands with their specific target receptor molecules can be examined and compared using binding free energy (kcal/mol). The tighter the receptor-ligand connection or the higher the binding affinity between the ligand and protein is indicated by the lowest binding energy and Ki value (Khan et al. 2016; Raj et al. 2019).

For this aim, we calculated the binding energy and inhibition constant (Ki) for the enzyme (collagenase) and compounds CTR-E1 (1,5-dicaffeoylquinic acid) and the positive control, EGCG by molecular docking analysis. The molecular interactions between CTR-E1 and the predicted active site of the selected enzyme were examined using molecular docking. The reference compound, EGCG also was evaluated to detect the same molecular interactions.

As a result of molecular docking analysis, CTR-E1, and the reference molecules were successfully docked with collagenase (Table 4). According to molecular docking studies, the maximum binding affinities for 1,5-dicaffeoylquinic acid and EGCG to collagenase were determined to be − 8.19 and − 6.98 kcal/mol, respectively. It was indicated that the Ki values of CTR-E1 and EGCG are 987,87 nM and 759 µM. CTR-E1 formed four hydrogen bonds with Trp539, Gly494 and Glu524 residues, and their atomic distances were 1.85 Å, 2.14 Å, 1.82 Å, respectively. As well as two pi-alkyl interactions with Ile497, Pro499 residues, and interacted carbon-hydrogen bond with GLU498 residue.

In addition, CTR-E1 formed a pi-sigma interaction at the Trp539 position 4.81 Å in length (Fig. 4). However, EGCG had seven conventional H bonds of length 1.85 Å, 2.06 Å, 2.78 Å, 2.19 Å, 3.00 Å; Glu559, Tyr496, Asp491, and Gly493 residue, respectively. Also, interactions with the pi-alkyl bond to Leu495 and pi-pi stacked interaction with His523 residue which belongs to the metal ion binding site of the enzyme were observed (Fig. 5). Consequently, It has been demonstrated that CTR-E1 (1,5-dicaffeoylquinic acid) binds to collagenase more potently than EGCG. The function of occupied residues by 1,5-dicaffeoylquinic acid as GLU498 (calcium metal binding site) and GLU524 (active site) was also explained for the collagenase (Nakanishi et al. 2000; Eckhard et al. 2013).

Conclusions

It has been discovered that six *Cirsium* species possess an inhibitory effect on collagenase. Additionally, CTR-E1 has been isolated from CT root using bio-activity guided fractionation studies, and in silico analysis has revealed interactions of CTR-E1 with collagenase. The most potent species, CT's root, was found to have a cytotoxic effect on SK-Mel. It has been discovered that the presence of CTR-E1 and the inhibition of collagenase may be responsible for the cytotoxic action. CT and its isolated bioactive compound, CTR-E1 possess therapeutic potential for the global health challenge of melanoma. The analysis performed through LC–MS/MS indicated that the compounds detected in CTR encompass 1,5-dicaffeoylquinic acid, along with fumaric acid, pyrogallol, and epicatechin, which demonstrate therapeutic potential for the treatment of melanoma. Consequently, It has been identified that CTR-E1 and standardized extracts of CT based on CTR-E1 represent promising candidates for the pharmacological management of melanoma. However, more research, clinical trials, and toxicological analyses are needed to support therapeutic efficacy.

Supplementary Information The online version contains supplementary material available at https://doi.org/10.1007/s11696-025-04149-7.

Acknowledgements We would like to acknowledge the Turkish Scientific and Technical Research Council for supporting the study (Project No. 116Z475, 215Z026). The study's authors, Sıla Özlem ŞENER and Şeyda KANBOLAT, also contributed additional financial support.

Author contributions Sila Ozlem Sener: Writing-Original Draft, Conceptualization, Methodology, Validation, Investigation, Formal Analysis, Supervision. Seyda Kanbolat: Writing—Review & Editing, Formal analysis, Merve Badem: Methodology, Validation, Investigation. Ufuk Özgen: Methodology, Supervision, Investigation. Rezzan Aliyazicioğlu: Methodology, Supervision, Investigation. Esma Ceylan: Methodology, Validation, Investigation. Ahmet Ceyhan Goren: Methodology, Validation. Tuncay Dirmenci: Resources. Turan Arabacı: Resources. Sermet Yıldırmış: Methodology, Investigation. Seyma Emiroğlu: Methodology, Investigation. Gülcin Saltan İscan: Methodology, Supervision.

Declarations

Conflict of interest All authors declare that they have no conflicts of interest.

References

Akkol EK, Süntar I, İlhan M, Aras E (2015) In vitro enzyme inhibitory effects of *Rubus sanctus* Schreber and its active metabolite as a function of wound healing activity. J Herb Med 5(4):207–210. https://doi.org/10.1016/j.hermed.2015.09.002

Ala-aho R, Kähäri VM (2005) Collagenases in cancer. Biochim 87(3–4):273–286. https://doi.org/10.1016/j.biochi.2004.12.009

AlQathama A, Prieto JM (2015) Natural products with therapeutic potential in melanoma metastasis. Nat Prod Rep 32(8):1170–1182. https://doi.org/10.1039/c4np00130c

Arnold M, Singh D, Laversanne M et al (2022) Global burden of cutaneous melanoma in 2020 and projections to 2040. JAMA Dermatol 158(5):495–503. https://doi.org/10.1001/jamadermatol.2022.0160

Badem M, Şener SÖ, Kanbolat Ş et al (2021) Evaluation of biological activities of *Barbarea integrifolia* and isolation of a new glucosinolate derivated compound. Z Für Naturforschung C 2021:1–8. https://doi.org/10.1515/znc-2020-0305

Berman HM, Westbrook J, Feng Z et al (2000) The protein data bank. Nucleic Acids Res 28:235–242. https://doi.org/10.1093/nar/28.1.235

Blackburn JS, Liu I, Coon CI et al (2009) A matrix metalloproteinase-1/protease activated receptor-1 signaling axis promotes melanoma invasion and metastasis. Oncogene 28(48):4237–4248. https://doi.org/10.1038/onc.2009.272

Brown PD (1997) Matrix metalloproteinase inhibitors in the treatment of cancer. Med Oncol 14(1):1–10. https://doi.org/10.1007/BF02990939

Chinembiri TN, Du Plessis LH, Gerber M, Hamman JH, du Plessis J (2014) Review of natural compounds for potential skin cancer treatment. Molecules 19(8):11679–11721. https://doi.org/10.3390/molecules190811679

Choi BM, Hong H, Park T et al (2022) Effects of luteolin-7-*O*-glucoside on melanin synthesis. J Appl Biol Chem 65(3):231–237. https://doi.org/10.1002/mnfr.201500822

Dassault Systèmes BIOVIA (2020) Discovery studio modeling environment. Dassault Systèmes, San Diego

Dirmenci T, Duman H, Arabacı T (2020) Türkiye'den yeni bir köygöçüren [Cirsium Mill. (Papatyagiller/Asteraceae)] türü ve cinsin şüpheli bir türünün yeniden keşfi. Bağbahçe Bilim Derg 7(3):35–44. https://doi.org/10.35163/bagbahce.730726

Domingues MRM, Domingues P, Reis A et al (2003) Identification of oxidation products and free radicals of tryptophan by mass spectrometry. JASMS 14(4):406–416. https://doi.org/10.1016/S1044-0305(03)00127-2

Duman H, Tugay O, Dirmenci T, Ertugrul K (2017) A new species of *Cirsium* sect. Epitrachys (Asteraceae: Cardueae) from the south of Turkey. Turk J Bot 41:375–387. https://doi.org/10.3906/bot-1612-33

Eckhard U, Schönauer E, Brandstetter H (2013) Structural basis for activity regulation and substrate preference of clostridial collagenases G, H, and T. J Biol Chem 288(28):20184–20194. https://doi.org/10.1074/jbc.M112.448548

Etemadi-Tajbakhsh N, Faramarzi MA, Delnavazi MR (2020) 1, 5-dicaffeoylquinic acid, an α-glucosidase inhibitor from the root of *Dorema ammoniacum* D. Don Res Pharm Sci 15(5):429–436. https://doi.org/10.4103/1735-5362.297845

EURACHEM/CITAC Guide CG 4 (2012) In: Ellison SLR, Williams A (Eds) Quantifying uncertainty in analytical measurement, 3rd edn

Gülçin İ, Gören AC, Taslimi P et al (2020) Anticholinergic, antidiabetic and antioxidant activities of anatolian pennyroyal (*Mentha pulegium*)-analysis of its polyphenol contents by LC–MS/MS. Biocatal Agric Biotechnol 23:1–10. https://doi.org/10.1016/j.bcab.2019.101441

Ha JH, Park SN (2018) Mechanism underlying inhibitory effect of six dicaffeoylquinic acid isomers on melanogenesis and the computational molecular modeling studies. BMCL 26(14):4201–4208. https://doi.org/10.1016/j.bmc.2018.07.014

Hofmann UB, Houben R, Bröcker EB, Becker JC (2005) Role of matrix metalloproteinases in melanoma cell invasion. Biochime 87(3–4):307–314. https://doi.org/10.1016/j.biochi.2005.01.013

Huaxi L, Zhuo L, Jingmei Y (2020) Liquid–liquid extraction process of amino acids by a new amide-based functionalized ionic liquid. Green Chem 14:1721–1727. https://doi.org/10.1039/C2GC16560K

Inafuku M, Nugara RN, Kamiyama Y et al (2013) *Cirsium brevicaule* A. GRAY leaf inhibits adipogenesis in 3T3-L1 cells and C57BL/6 mice. Lipids Health Dis 12:124–133. https://doi.org/10.1186/1476-511X-12-124

Jurrus E, Engel D, Star K et al (2018) Improvements to the APBS biomolecular solvation software suite. Prot Sci 27(1):112–128. https://doi.org/10.1002/pro.3280

Kerkelä E, Saarialho-Kere U (2003) Matrix metalloproteinases in tumor progression: focus on basal and squamous cell skin cancer. Exp Dermatol 12(2):109–125. https://doi.org/10.1034/j.1600-0625.2003.120201.x

Khan FI, Wei DQ, Gu KR, Hassan MI, Tabrez S (2016) Current updates on computer aided protein modeling and designing. Int J Biol Macromol 85:48–62. https://doi.org/10.1016/j.ijbiomac.2015.12.072

Khan NH, Mir M, Qian L et al (2021) Skin cancer biology and barriers to treatment: recent applications of polymeric micro/nanostructures. J Adv Res 36:223–247. https://doi.org/10.1016/j.jare.2021.06.014

Kim HJ, Lee YS (2005) Identification of new dicaffeoylquinic acids from *Chrysanthemum morifolium* and their antioxidant activities. Planta Med 71(9):871–876. https://doi.org/10.1055/s-2005-873115

Kim S, Chen J, Cheng T et al (2023) PubChem 2023 update. Nucleic Acids Res 51:1373–1380. https://doi.org/10.1093/nar/gkac956

Kiziltas H, Bingol Z, Goren AC et al (2022) Comprehensive metabolic profiling of *Acantholimon caryophyllaceum* using LC–HRMS and evaluation of antioxidant activities, enzyme inhibition properties and molecular docking studies. S Afr J 151:743–755. https://doi.org/10.1016/j.sajb.2022.10.048

Kozyra M, Głowniak K (2013) Phenolic acids in extracts obtained from the flowering herbs of *Cirsium vulgare* (Savi) Ten. growing in Poland. Acta Soc Bot Pol 82:325–329. https://doi.org/10.5586/asbp.2013.039

Lida J, McCarthy JB (2007) Expression of collagenase-1 (MMP-1) promotes melanoma growth through the generation of active transforming growth factor-β. Melanoma Res 17(4):205–213. https://doi.org/10.1097/CMR.0b013e3282a660ad

Llorent-Martínez EJ, Zengin G, Sinan KI et al (2020) Impact of different extraction solvents and techniques on the biological activities of *Cirsium yildizianum* (Asteraceae: Cynareae). Ind Crops Prod 144:1–8. https://doi.org/10.1016/j.indcrop.2019.112033

Loewe R, Valero T, Kremling S (2006) Dimethylfumarate impairs melanoma growth and metastasis. Cancer Res 66(24):11888–11896. https://doi.org/10.1158/0008-5472.CAN-06-2397

Malta LFB, Senra JD, Tinoco LW et al (2009) Chiral Recognition of 2-hydroxypropyl-alpha-cyclodextrin towards DLTryptophan. Lett Org Chem 6:258–263. https://doi.org/10.2174/157017809787893091

Morris GM, Huey R, Lindstrom W et al (2009) AutoDock4 and AutoDockTools4: automated docking with selective receptor flexibility. J Comput Chem 30:2785–2791. https://doi.org/10.1002/jcc.21256

Nakanishi I, Kinoshita T, Sato A et al (2000) Structure of porcine pancreatic elastase complexed with FR901277 a novel macrocyclic inhibitor of elastases at 1.6 Å resolution. Biopolym Orig Res Biomole 53(5):434–445. https://doi.org/10.1002/(SICI)1097-0282(20000415)53:5%3c434::AID-BIP7%3e3.0.CO;2-5

Napoli S, Scuderi C, Gattuso G et al (2020) Functional roles of matrix metalloproteinases and their inhibitors in melanoma. Cells 9(5):1–23. https://doi.org/10.3390/cells9051151

Nazaruk J (2014) Galicka A (2014) The influence of selected flavonoids from the leaves of *Cirsium palustre* (L.) Scop. On collagen expression in human skin fibroblasts. Phytother Res 28(9):1399–1405. https://doi.org/10.1002/ptr.5143

Nguyen V, Taine EG, Meng D, Cui T, Tan W (2024) Chlorogenic acid: a systematic review on the biological functions, mechanistic actions, and therapeutic potentials. Nutrients 16(7):1–36. https://doi.org/10.3390/nu16070924

Oh JH, Karadeniz F, Kong CS et al (2020) Antiphotoaging effect of 3, 5-dicaffeoyl-epi-quinic acid against UVA-induced skin damage by protecting human dermal fibroblasts in vitro. Int J Mol Sci 21(20):1–12. https://doi.org/10.3390/ijms21207756

Popescu D, El-Khatib M, El-Khatib H, Ichim L (2022) New trends in melanoma detection using neural networks: a systematic review. Sensors 22(2):1–41. https://doi.org/10.3390/s22020496

Raj S, Sasidharan S, Dubey VK, Saudagar P (2019) Identification of lead molecules against potential drug target protein MAPK4 from L. *donovani*: an *in-silico* approach using docking, molecular dynamics and binding free energy calculation. PLoS ONE 14(8):1–20. https://doi.org/10.1371/journal.pone.0221331

Saginala K, Barsouk A, Aluru JS, Rawla P, Barsouk A (2021) Epidemiology of melanoma. Med Sci 9(4):1–9. https://doi.org/10.3390/medsci9040063

Şener SÖ, Özgen U, Kanbolat Ş (2021) Investigation of therapeutic potential of three endemic *Cirsium* species for global health problem obesity. S Afr J Bot 141:243–254. https://doi.org/10.1016/j.sajb.2021.05.004

Seyhan MF, Yılmaz E, Timirci-Kahraman Ö et al (2019) Different propolis samples, phenolic content, and breast cancer cell lines: variable cytotoxicity ranging from ineffective to potent. IUBMB Life 71(5):619–631. https://doi.org/10.1002/iub.1996

Silva ATM, Magalhães CG, Duarte LP et al (2017) Lupeol and its esters: NMR, powder XRD data and in vitro evaluation of cancer cell growth. Braz J Pharm Sci 53(3):1–10. https://doi.org/10.1590/s2175-97902017000300251

Sim GS, Kim JH, Lee DH et al (2007) The inhibition of UVA-induced matrix metalloproteinase-1 in human dermal fibroblasts and the improvement of skin elasticity by *Cirsium setidens* extract. J Soc Cosmet Sci Korea 33(3):181–187

Singh J (1996) International conference on harmonization (ICH) of technical requirements for the registration of pharmaceuticals for human use validation of analytical procedures. In: Methodology, ICH-Q2B, Geneva

Smith D (2017) Fumaric acid esters for psoriasis: a systematic review. Ir J Med Sci 186:161–177. https://doi.org/10.1007/s11845-016-1470-2

Thring TS, Hili P, Naughton DP (2009) Anti-collagenase, anti-elastase and anti-oxidant activities of extracts from 21 plants. BMC Complement Altern Med 9(1):1–11. https://doi.org/10.1186/1472-6882-9-27

Tian W, Chen C, Lei X, Zhao J, Liang J (2018) CASTp 3.0: computed atlas of surface topography of proteins. Nucleic Acids Res 46:363–367. https://doi.org/10.1093/nar/gky473

Tolonen A, Joutsamo T, Mattlla S, Kämäräinen T, Jalonen J (2002) Identification of isomeric dicaffeoylquinic acids from *Eleutherococcus senticosus* using HPLC-ESI/TOF/MS and ^{1}H-NMR methods. Phytochem Anal 13(6):316–328. https://doi.org/10.1002/pca.663

Upadhyay G, Gupta SP, Prakash O (2010) Pyrogallol-mediated toxicity and natural antioxidants: triumphs and pitfalls of preclinical findings and their translational limitations. Chem Biol Interact 183(3):333–340. https://doi.org/10.1016/j.cbi.2009.11.028

Widowati W, Wargasetia TL, Rahardja F (2024) Potential of epicatechin as antioxidant and antiaging in UV-induced BJ cells by regulating COL1A1, FGF-2, GPX-1, and MMP-1 gene, protein levels, and apoptosis. PeerJ 12:1–19. https://doi.org/10.7717/peerj.18382

Yeşilada E, Honda G, Sezik E et al (1995) Traditional medicine in Turkey. V. Folk medicine in the inner Taurus mountains. J Ethnopharmacol 46:133–152. https://doi.org/10.1016/0378-8741(95)01241-5

Yoon S, Kim M, Shin S et al (2022) Effect of *Cirsium japonicum* flower extract on skin aging ınduced by glycation. Molecules 27(7):1–14. https://doi.org/10.3390/molecules27072093

Zhang L, Shi J, Feng J, Klocker H, Lee J, Zhang J (2004) Type IV collagenase (matrix metalloproteinase-2 and -9) in prostate cancer. Prostate Cancer Prostatic Dis 7:327–332. https://doi.org/10.1038/sj.pcan.4500750

Zheng Z, Wang X, Liu P, Li M, Dong H, Qiao X (2018) Semi-preparative separation of 10 caffeoylquinic acid derivatives using high speed counter-current chromatogaphy combined with semi-preparative HPLC from the roots of burdock (*Arctium lappa L.*). Molecules 23(2):1–11. https://doi.org/10.3390/molecules23020429